Electronic Supplementary Information

Synthesis, biological evaluation, substitution behaviour and DFT study of Pd(II) complexes incorporating benzimidazole derivative

Ishani Mitra[a], Subhajit Mukherjee[a], Venkata P. Reddy B.[a], Bashkim Misini[b], Payel Das[c], Subrata Dasgupta[a], Wolfgang Linert[b] and Sankar Ch. Moi*[a]

a. Department of Chemistry, National Institute of Technology, Durgapur-713209, W.B. India
b. Institute of Applied Synthetic Chemistry, Vienna University of Technology, Getreidemarkt, 9/163-AC, 1060 Vienna, Austria
c. Department of Biotechnology, National Institute of Technology, Durgapur-713209, W.B. India

Table of contents

		the presence of increasing amounts of CT-DNA (0–200 μM). The arrow indicates the chenges in the absorbance on addition of DNA. Inset: linear fit of [DNA]/(ε_a - ε_f) vs. [DNA].
27	SUP. Fig. S27	Emission spectra for EB–DNA ([EB] = 20 μM, [DNA] = 20 μM) in the absence and presence of increasing amounts of (A) **C3** (B) **C4** (C) **C5** and (D) **C6**. The arrow shows the changes of intensity upon increasing amount of complexes. Inset: Plot of I_0/I versus [complex].
28	SUP. Fig. S28	Scatchard plot for DNA binding of complexes **C1**-**C6**.
29	SUP. Fig. S29	Effect of increasing amounts of EB and studied Pd(II) complexes on the relative viscosity of CT-DNA at 25^{o}C.
30	SUP. Fig. S30	Computational docking models illustrating the interactions of (A) **C3** , (B) **C4**, (C) **C5** with 1DNE and of (D) **C6** with 1DSC.
31	SUP. Fig. S31	Magnified view of the docked models showing the interaction of complexes **C1**-**C6** with DNA base pairs.
32	SUP. Fig. S32	Absorption spectra of BSA (10 μM) in Tris-HCl buffer in presence of the complexes **C1–C6** (5 μM).
33	SUP. Fig. S33	Emission spectra of BSA (1.0 μM) in Tris-HCl buffer(pH 7.0) at 298 K in presence of (A) **C1**, (B) **C3** and (C) **C4** (5-60 μM). The arrow shows the emission intensity changes upon increasing complex concentration. Insets: Stern-Volmer plot showing tryptophan quenching in BSA.
34	SUP. Fig. S34	Scatchard plot for BSA binding of complexes **C1**-**C6**.
35	SUP. Fig. S35	Growth Inhibition (%) of MDA-MB-231, A549, and HepG2 cell lines in presence of complex **C1**-**C6** and Cisplatin (5-50 μM).
36	SUP. Table S1	10^{-3} ×$k_{1(obs)}$ (s^{-1}) and $k_{2(obs)}$ (s^{-1}) values at different [ligand] at different temperatures; [**C2**] = 4.71 ×10^{-4} M, pH = 4.0, ionic strength = 0.1 M $NaClO_4$ (Herein **"**± values" represent standard error values)
37	SUP. Table S2	Energy and composition of some selected MOs of **C3**-**C6**.
38	SUP. Table S3	Occupancy (e) and polarity (%) of natural bond orbitals (NBOs) and hybrids calculated for complex **C4**-**C6**.
39	SUP. Table S4	Selected vertical excitations calculated by TDDFT/B3LYP/6-31G(d)/6-31G+(d)/LANL2DZ /CPCM/water for **C3**-**C6**.
40	SUP. Table S5	Band shift (nm) and free energy (kJ mol^{-1}) of DNA binding by absorption titration.
41	SUP. Table S6	Hydrogen bonding interactions and the binding free energy of the most stable docking conformations for complexes **C1**–**C6** docked into DNA.
42	SUP. Table S7	IC_{50} values (in μM) of the complexes **C1**-**C6** and cisplatin on different cancer cell lines for 48 hrs incubation.
43	SUP. Equation S1	Wolfe-Shimer equation
44	SUP. Equation S2	Free energy of binding
45	SUP. Equation S3	Stern–Volmer equation
46	SUP. Equation S4	Scatchard equation

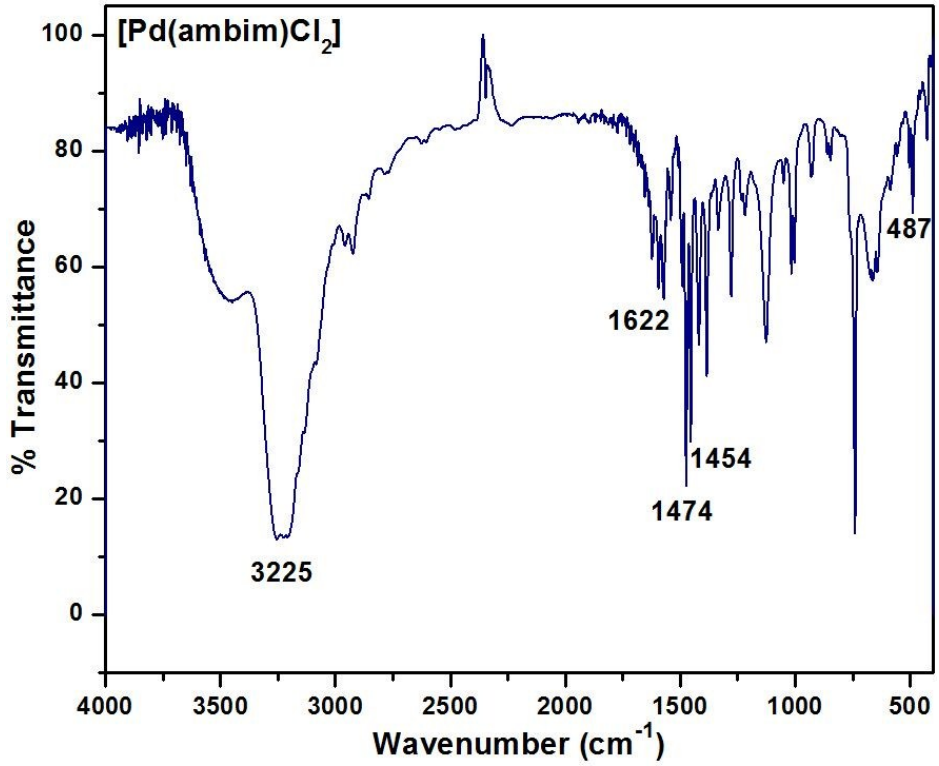

Sup. Fig. S1 IR spectrum of **C1**

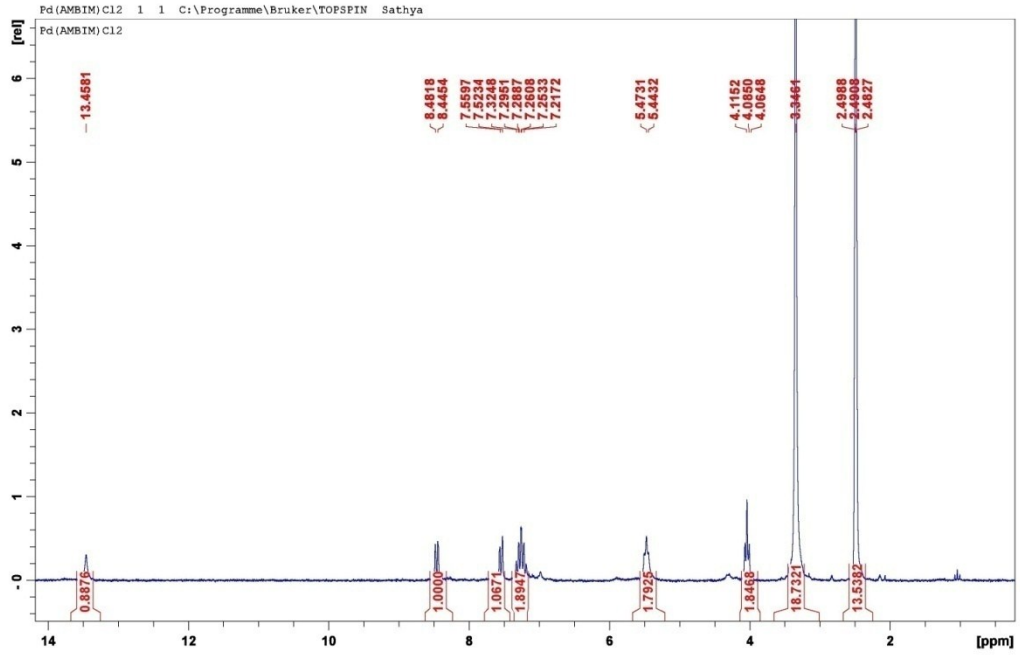

Sup. Fig. S2 ^{1}H NMR spectrum of **C1** in DMSO-D_6

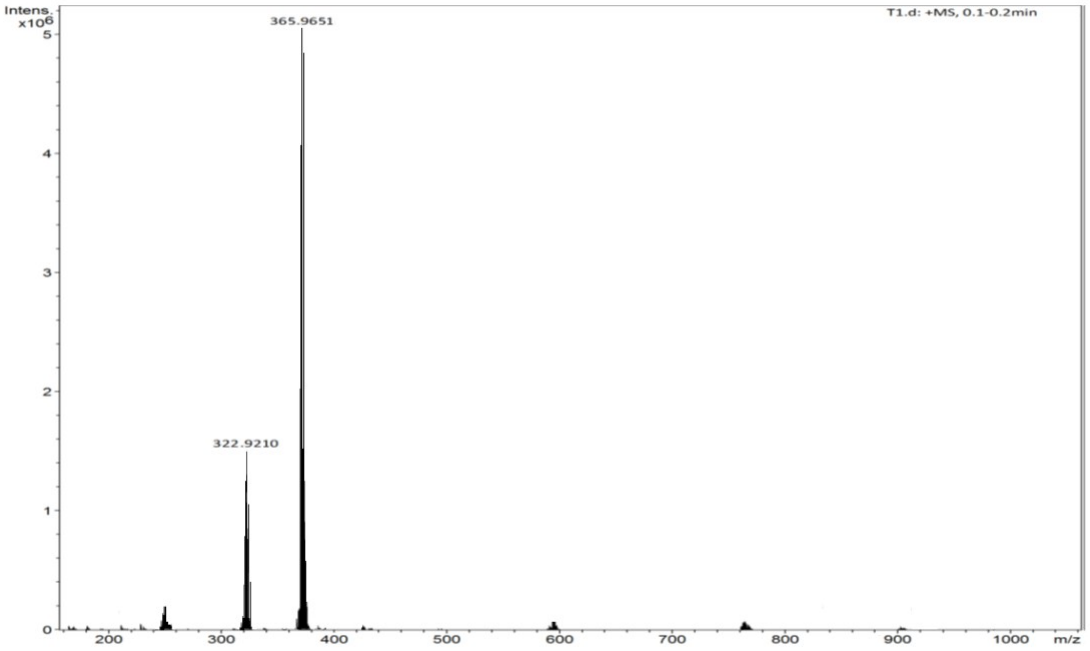

Sup. Fig. S3 ESI-Mass spectrum of **C1** in DMSO

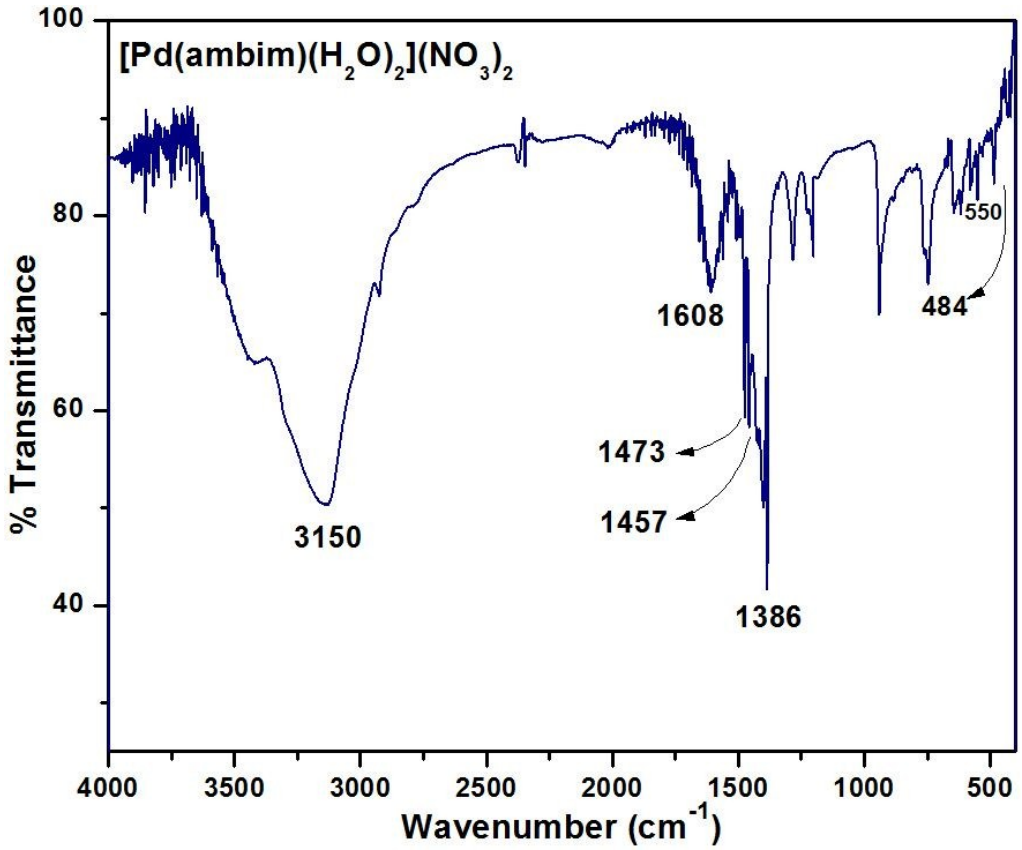

Sup. Fig. S4 IR spectrum of **C2**

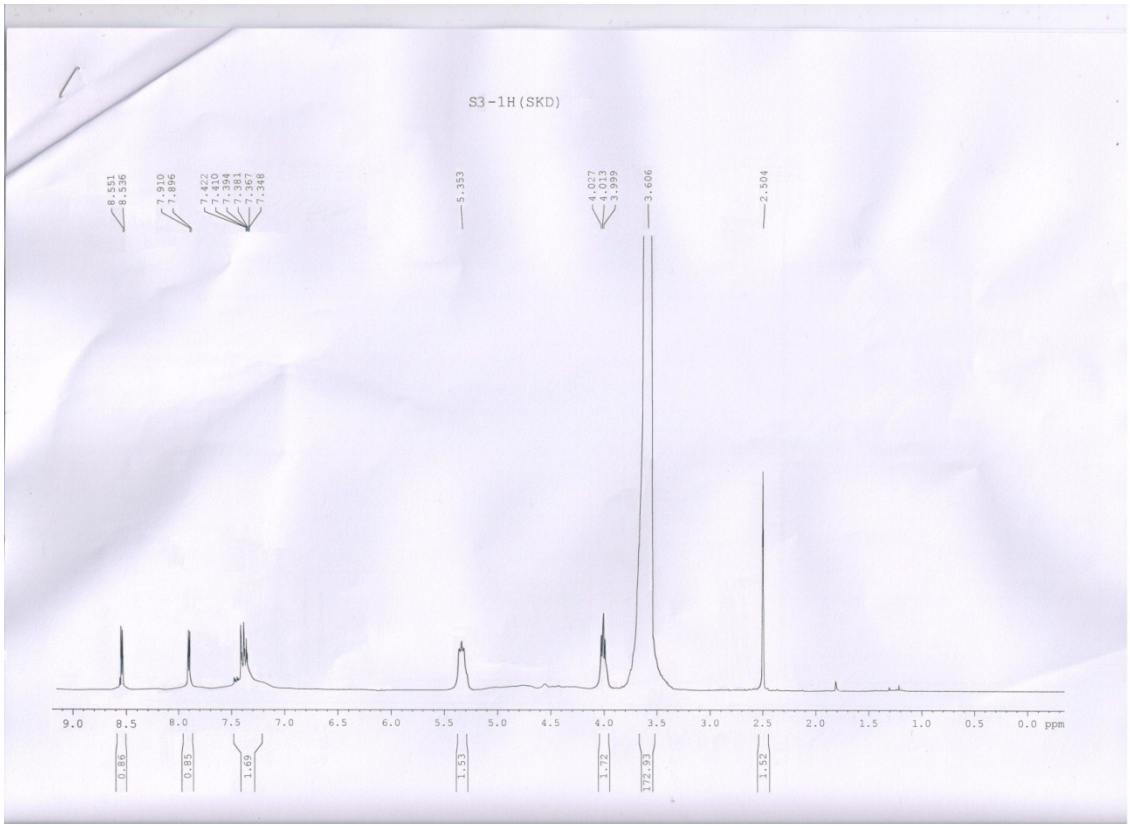

Sup. Fig. S5 ^{1}H NMR spectrum of **C2** in mixed solvent DMSO-D_6

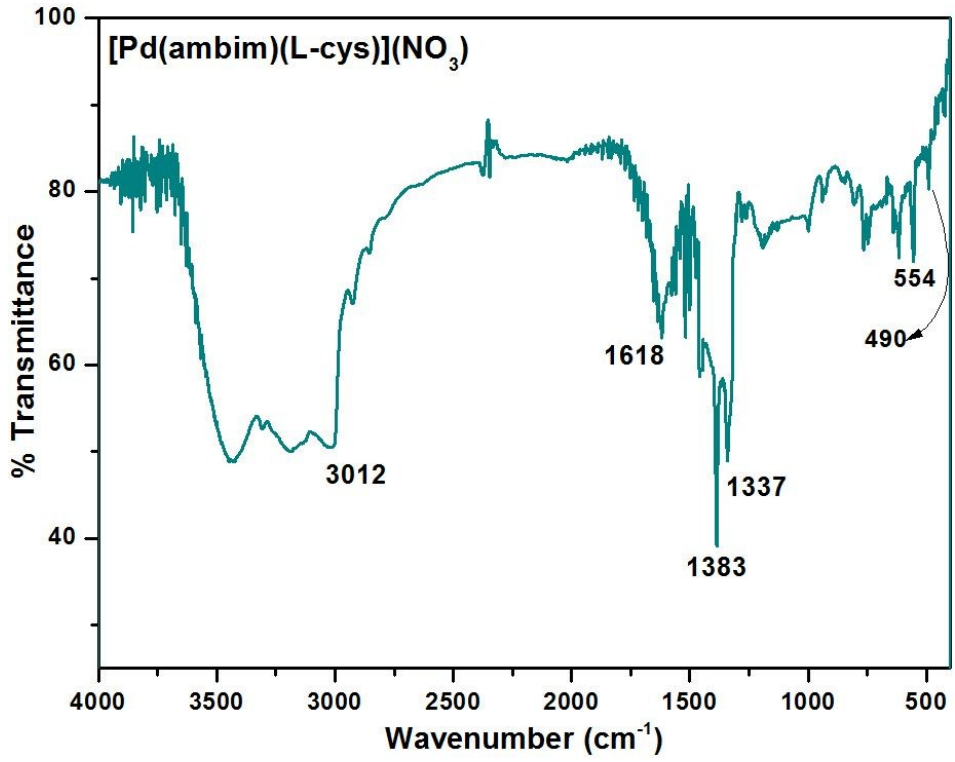

Sup. Fig. S6 IR spectrum of **C3**

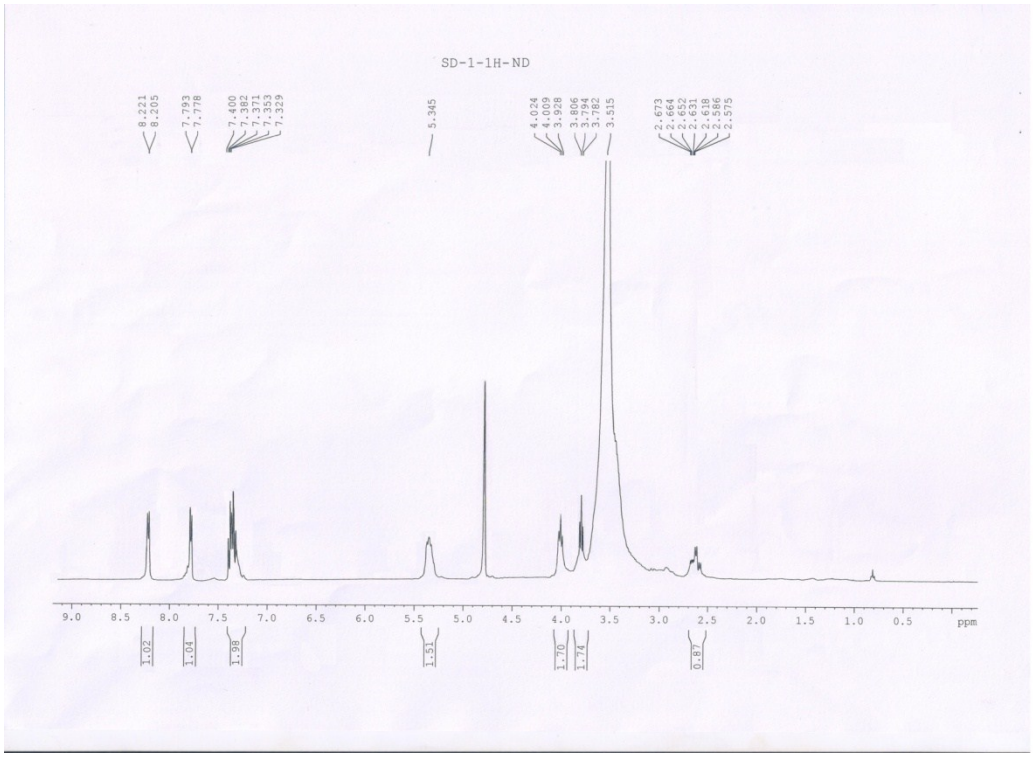

Sup. Fig. S7 ^{1}H NMR spectrum of **C3** in D_2O

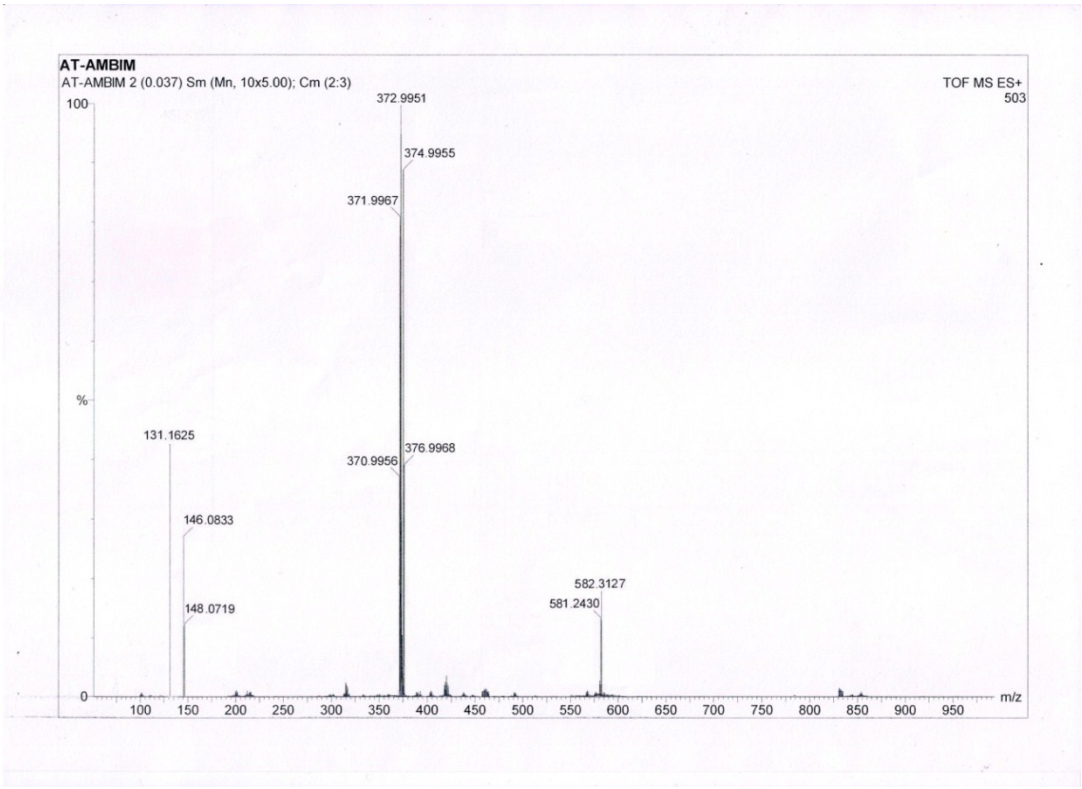

Sup. Fig. S8 ESI-Mass spectrum of **C3** in water

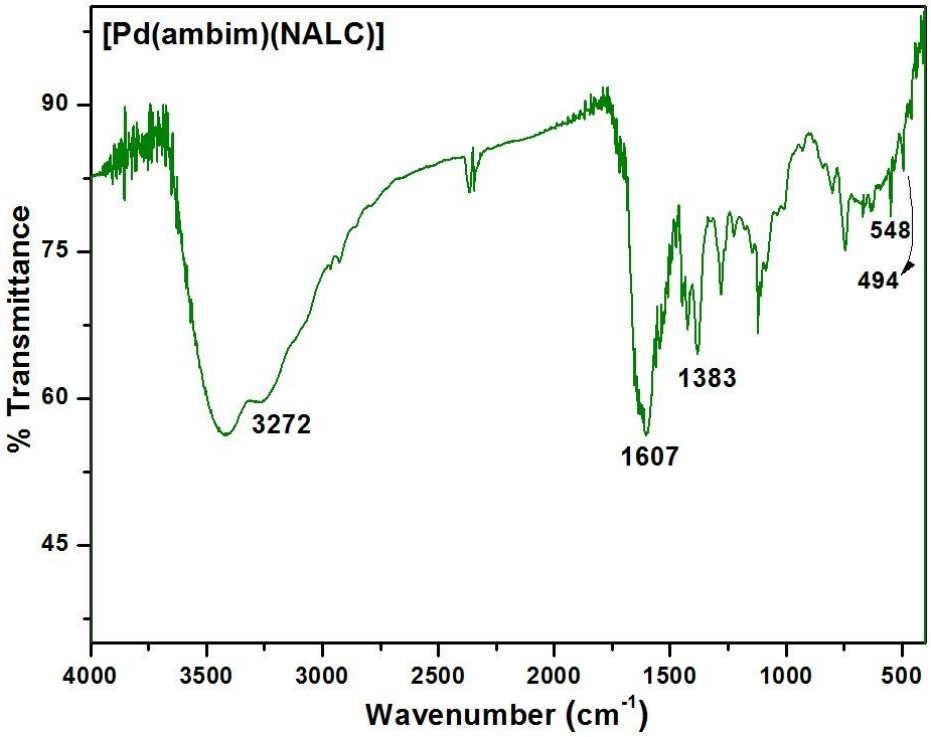

Sup. Fig. S9 IR spectrum of **C4**

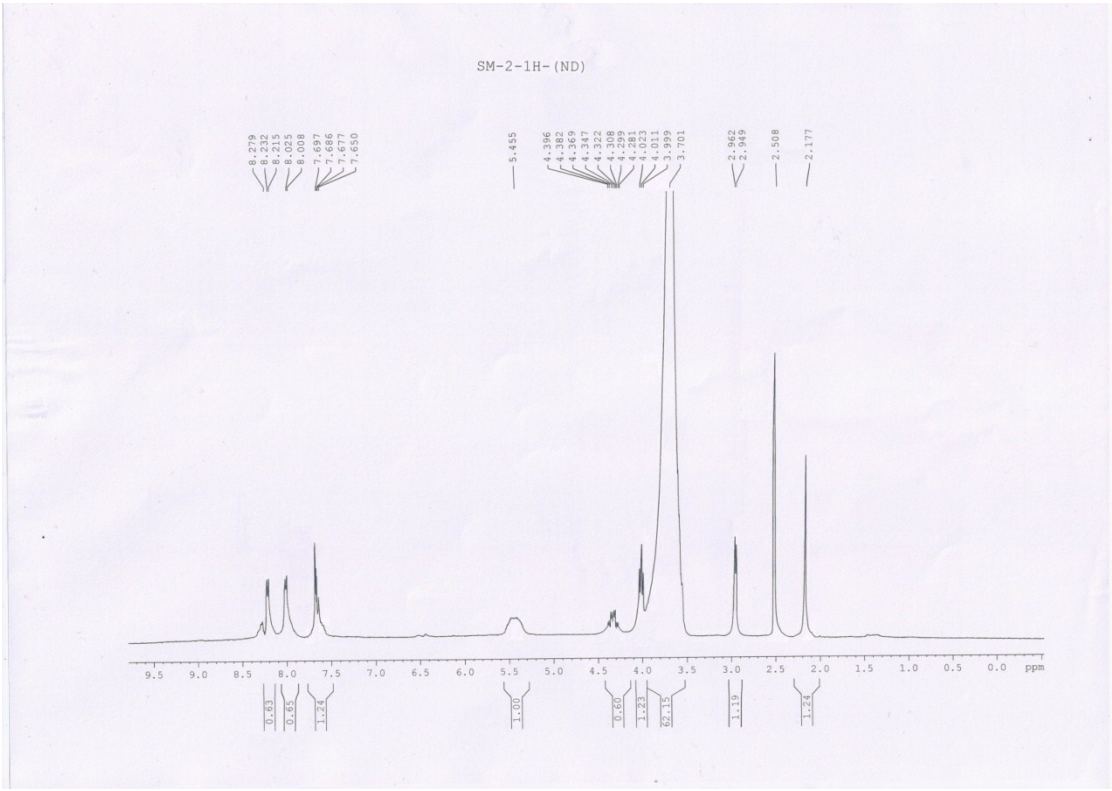

Sup. Fig. S10 ^{1}H NMR spectrum of **C4** in DMSO-D_6

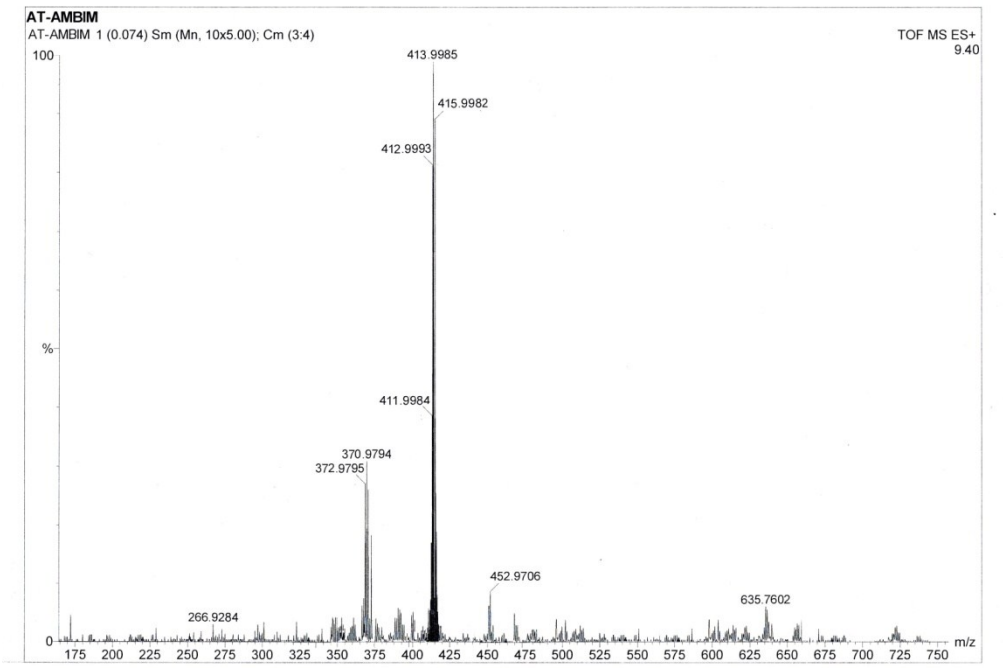

Sup. Fig. S11 ESI-Mass spectrum of **C4** in water

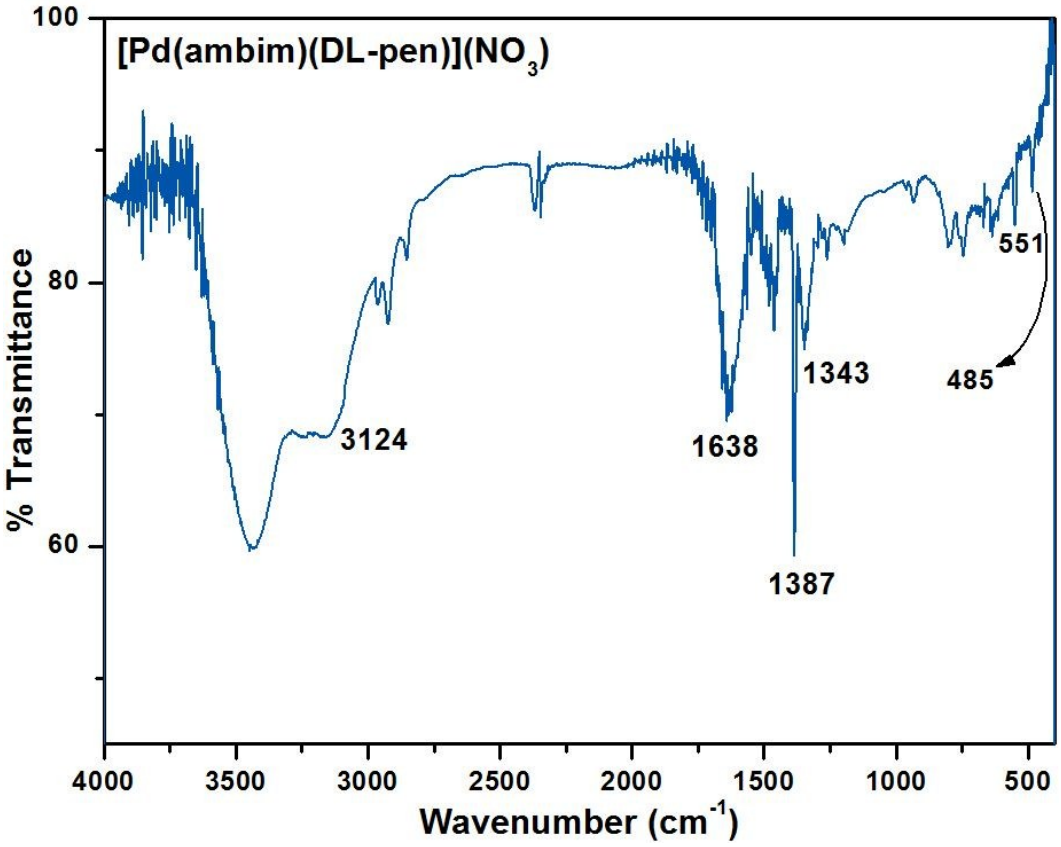

Sup. Fig. S12 IR spectrum of **C5**

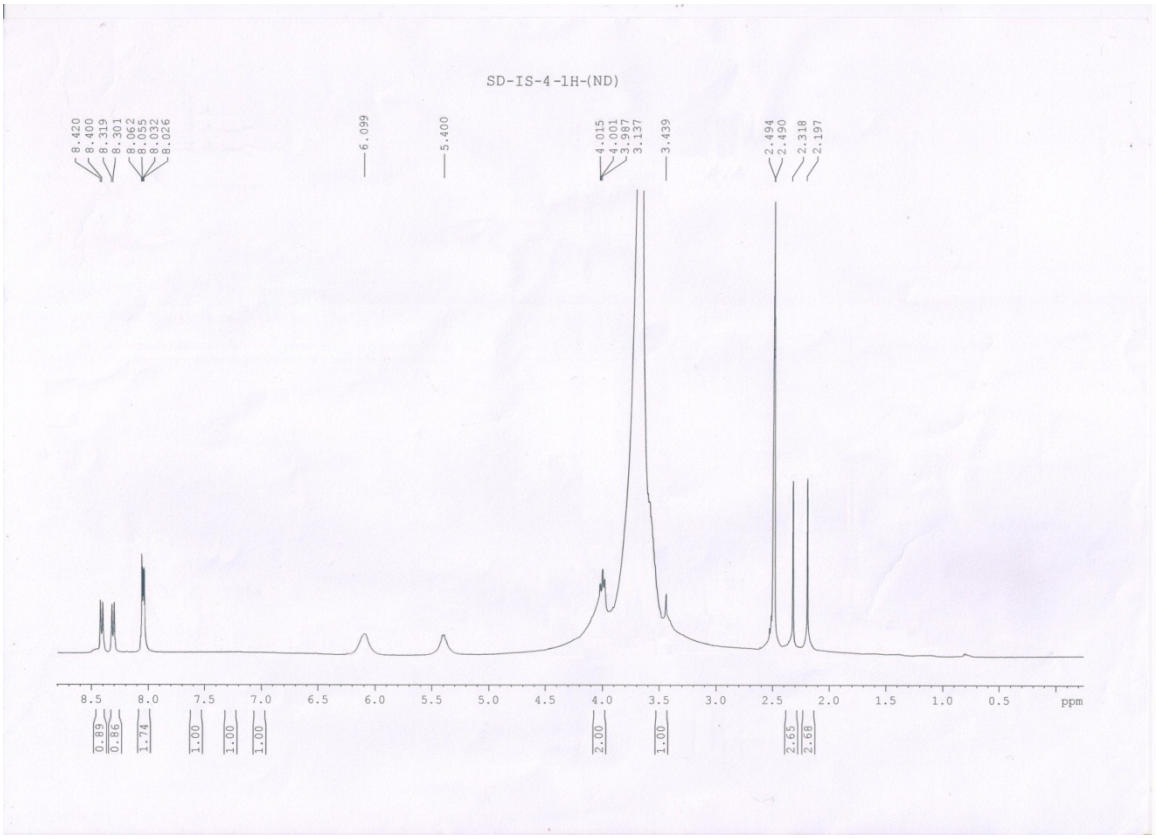

Sup. Fig. S13 ^{1}H NMR spectrum of **C5** in DMSO-D_6

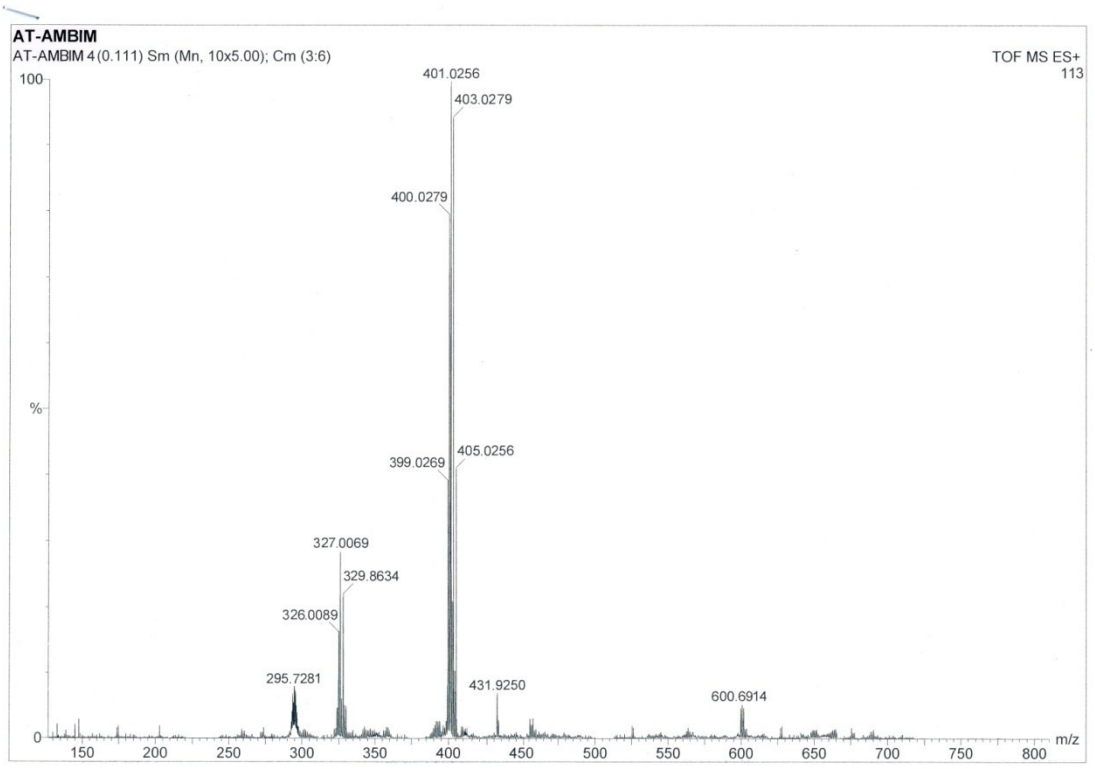

Sup. Fig. S14 ESI-Mass spectrum of **C5** in water

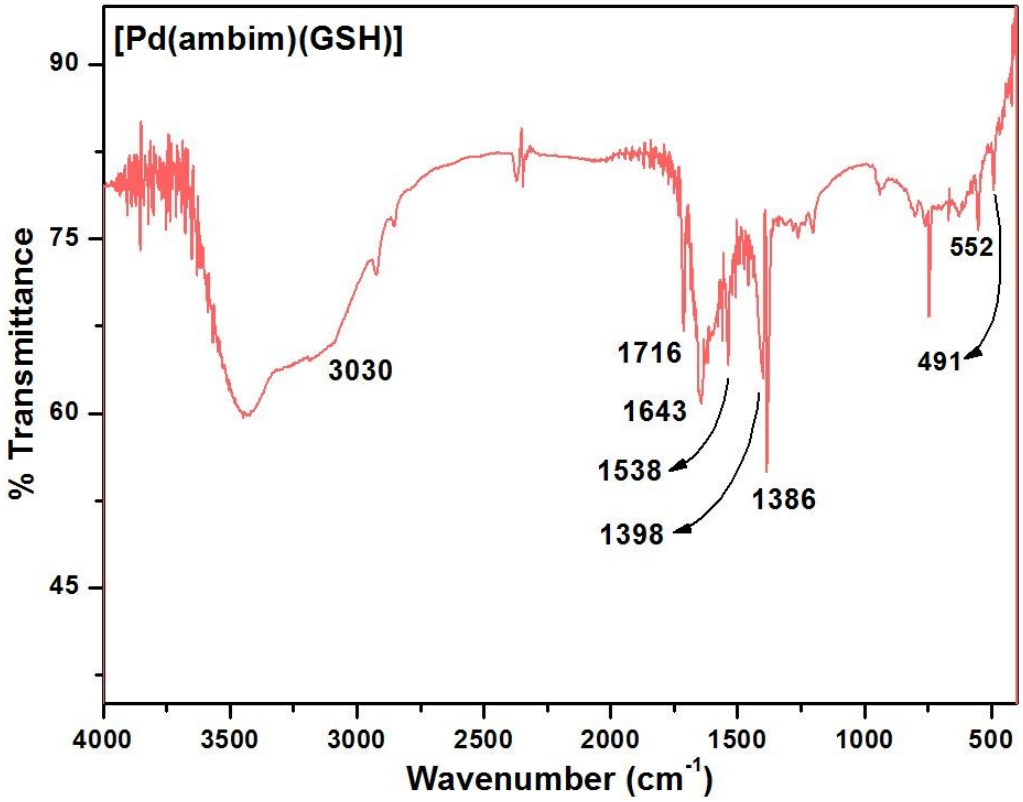

Sup. Fig. S15 IR spectrum of **C6**

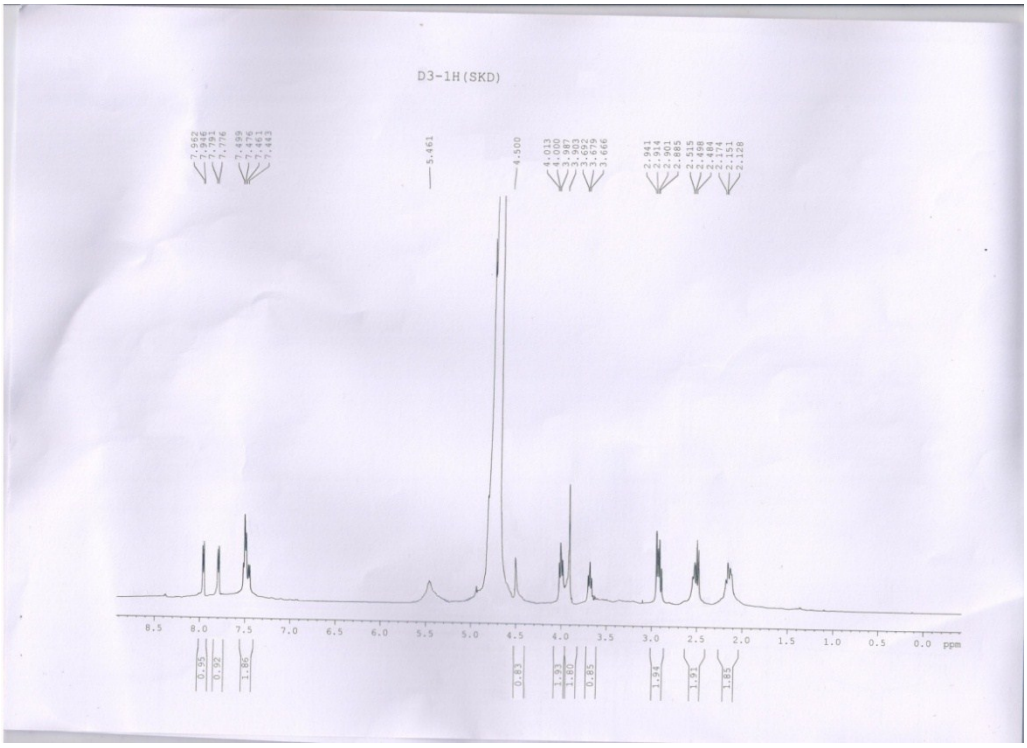

Sup. Fig. S16 ^{1}H NMR spectrum of **C6** in D_2O

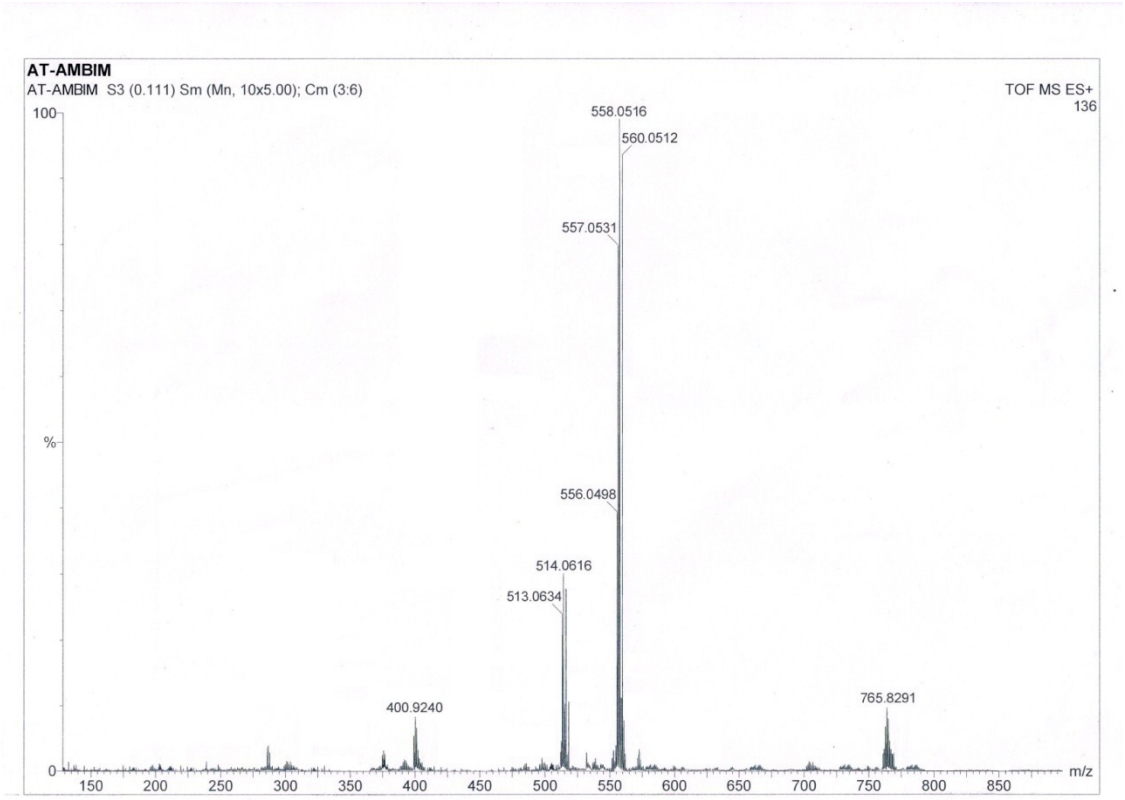

Sup. Fig. S17 ESI-Mass spectrum of **C6** in water

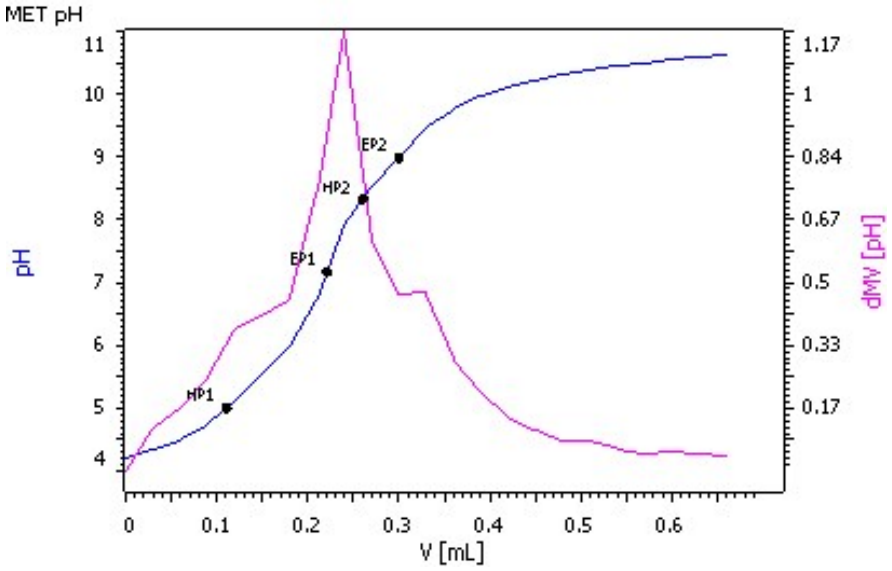

Sup. Fig. S18 Plot of pH vs volume (mL) for the titration of 1.00×10^{-4} M solution of **C2** using standard 0.025 M KOH.

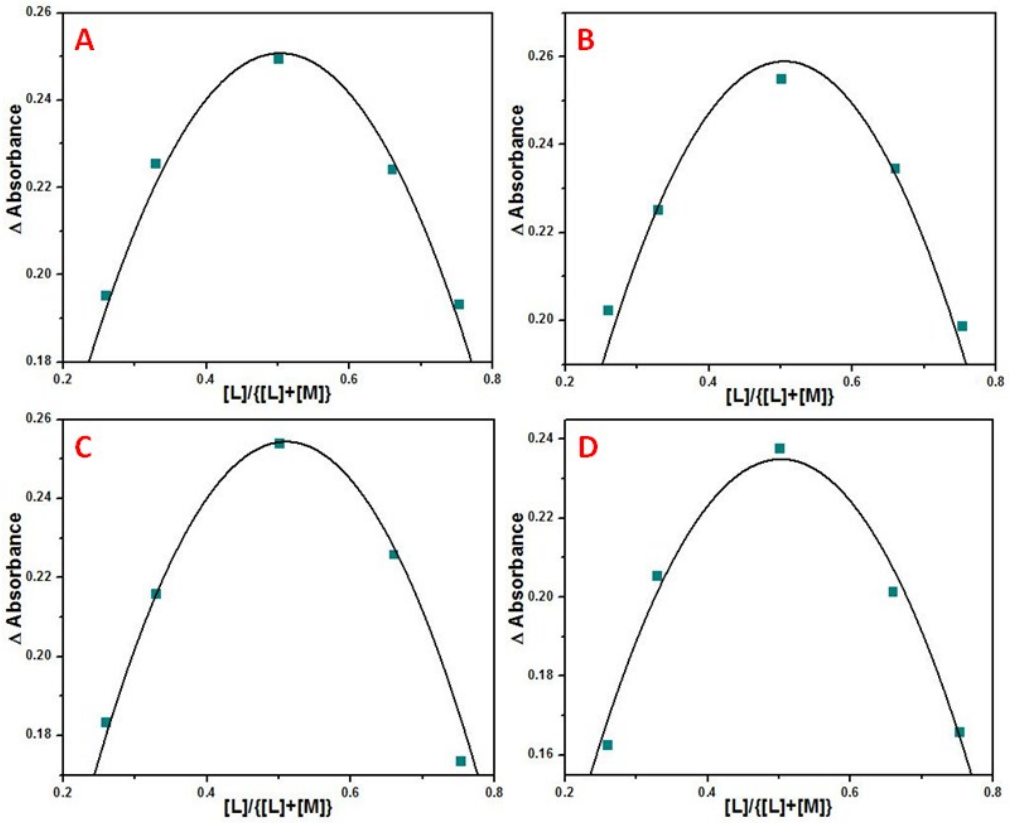

Sup. Fig. S19 Job's plot for the formation of complexes **C3**-**C6** at pH 4.0.

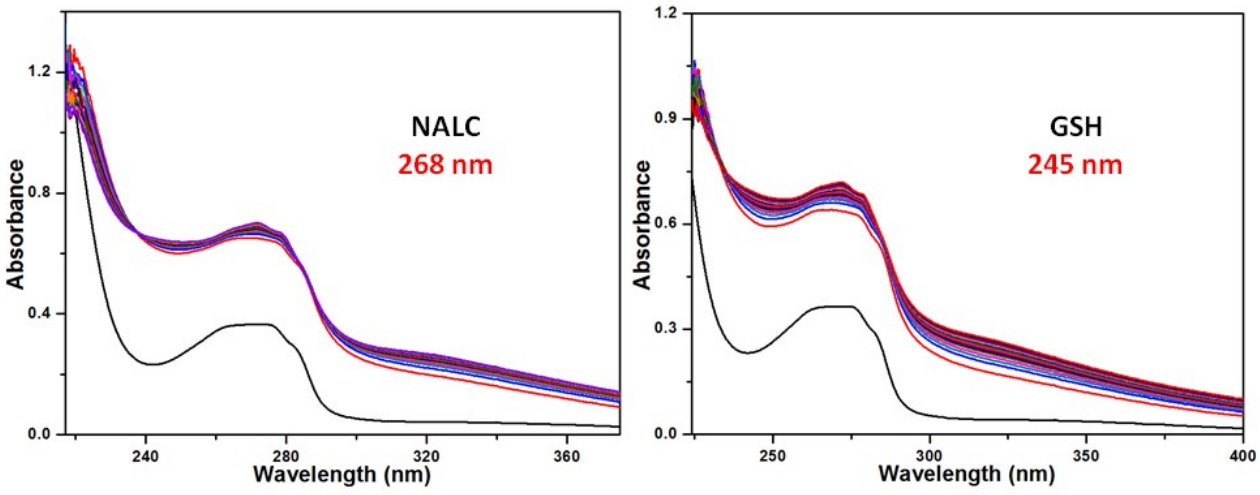

Sup. Fig. S20 Scan overlay at 2-min interval of the reaction of **C2** with NALC and GSH. [**C2**] = 4.71 x 10^{-4} M, [NALC/GSH] = 4.71 x 10^{-3} M, pH = 4.0, 25 ^{o}C.

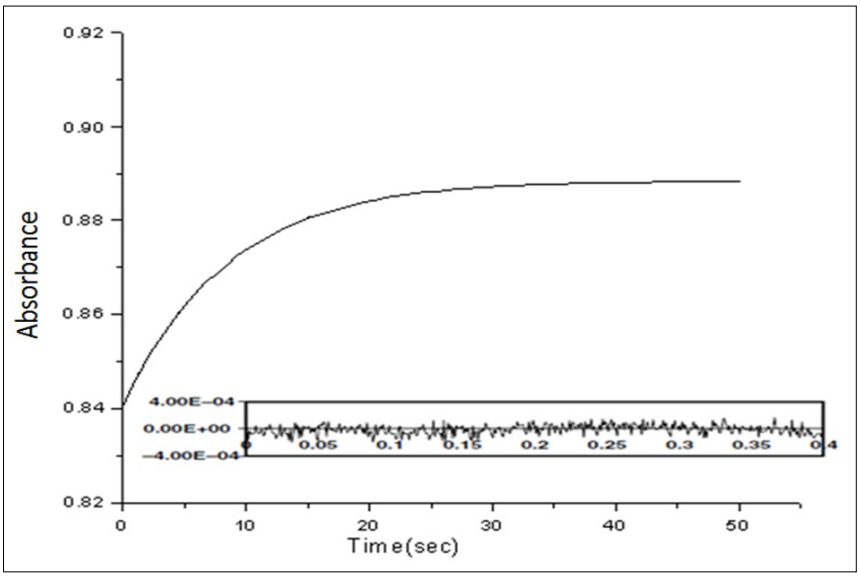

Sup. Fig. S21 Typical absorbance-time trace for the reaction of **C2** with L-cys fitted with two exponential functions. The top of the figure shows the absorbance difference between measured and calculated kinetic traces. [**C2**] =4.71× 10^{-4} M; [L-cys] = 4.71× 10^{-3} M; pH = 4.0, λ = 250 nm; T = 25 °C.

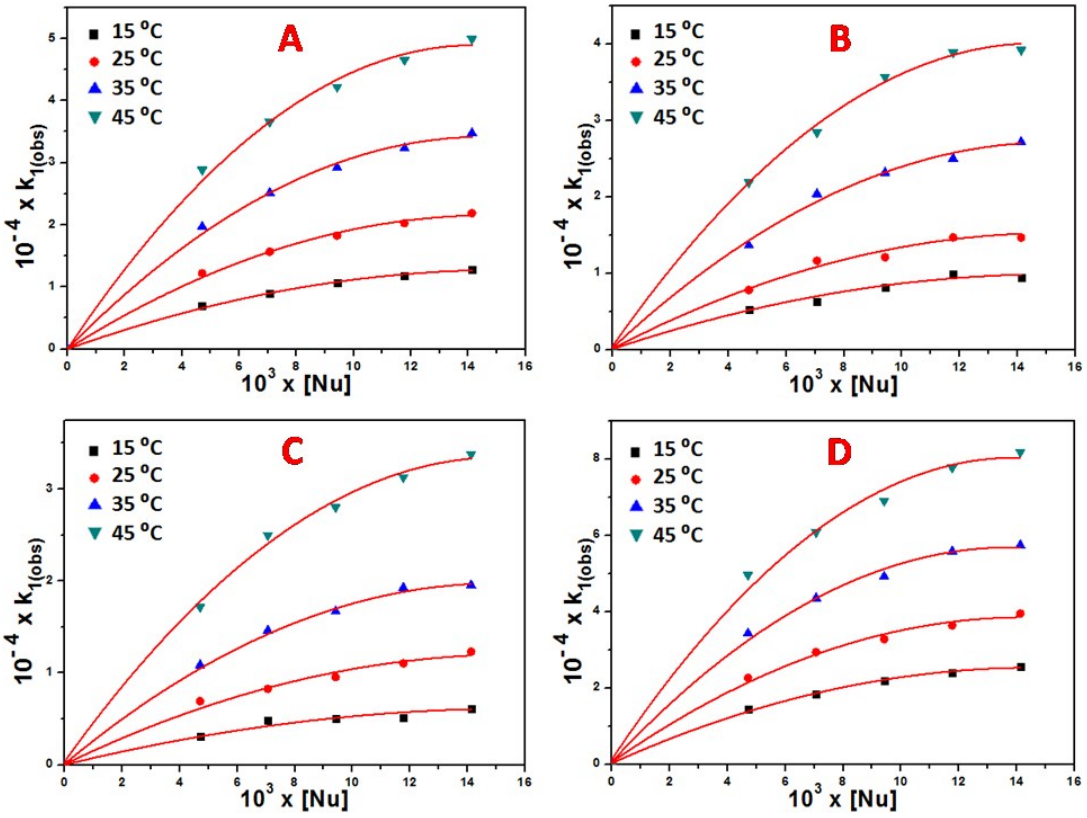

Sup. Fig. S22 Plot of $10^{-4} \times k_{1(obs)}$ versus $10^{3} \times$ [Nu] at different temperatures. (A) L-cys, (B) NALC, (C) DL-pen, (D) GSH

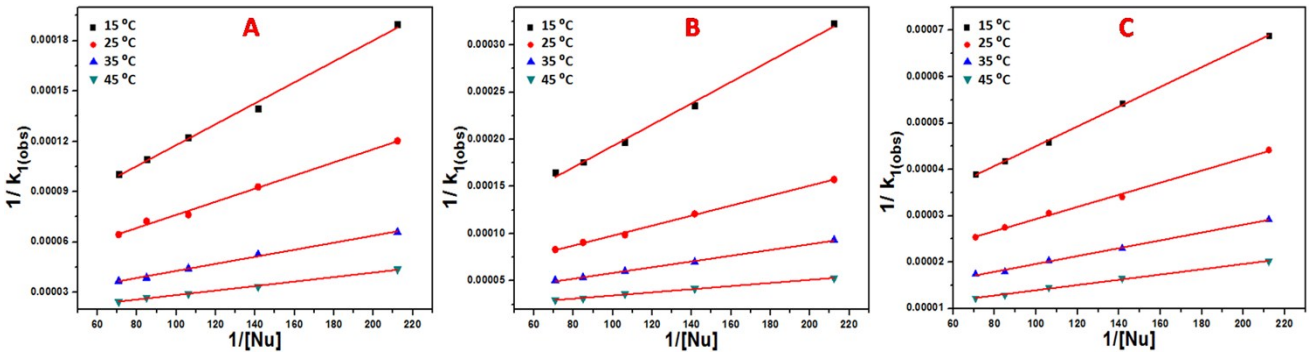

Sup. Fig. S23 Plot of 1/ $k_{1(obs)}$ versus 1/ [Nu] at different temperatures. (A) NALC, (B) DL-pen, (C) GSH

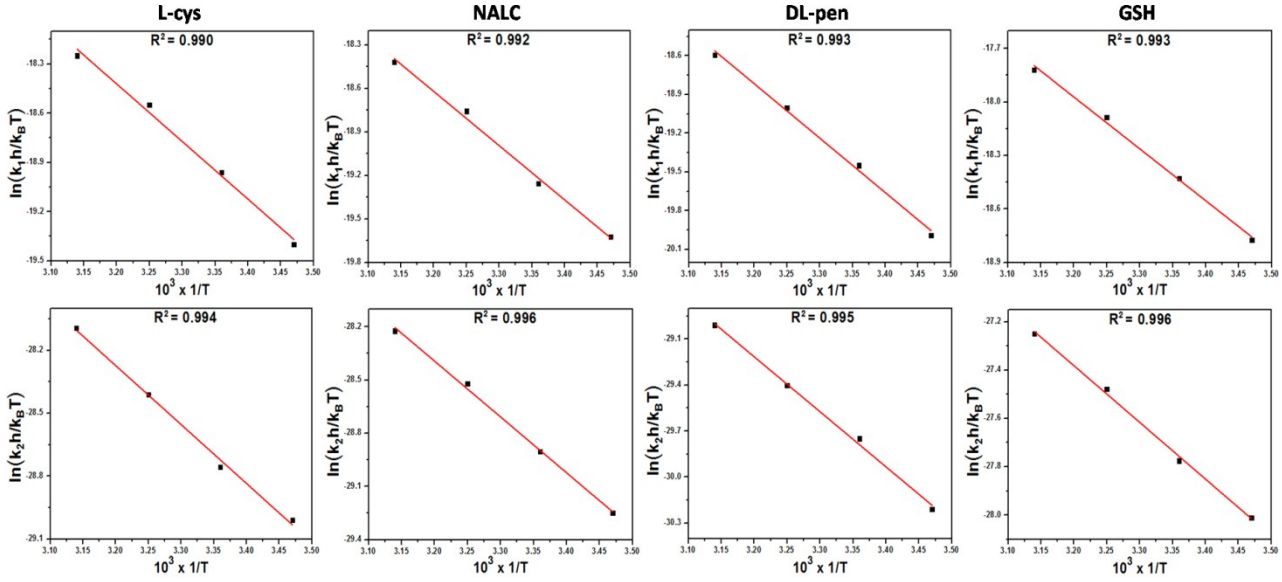

Sup. Fig. S24 Eyring plots (ln k_1h/k_BT vs $10^3 \times 1/T$ and ln k_2h/k_BT vs $10^3 \times 1/T$) for the reaction of **C2** with L-cys, NALC, DL-pen and GSH.

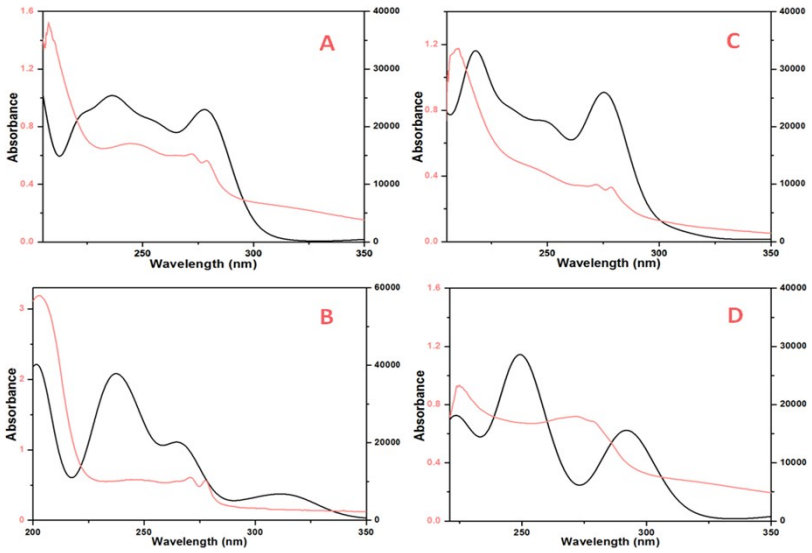

Sup. Fig. S25 Experimental (in pink) and simulated (in black) UV-Vis spectrum of the Pd(II) complexes **C3**-**C6** in CPCM/water (Simulation done at TDDFT/B3LYP/6-31G(d)/6-31G+(d)/LANL2DZ level of theory).

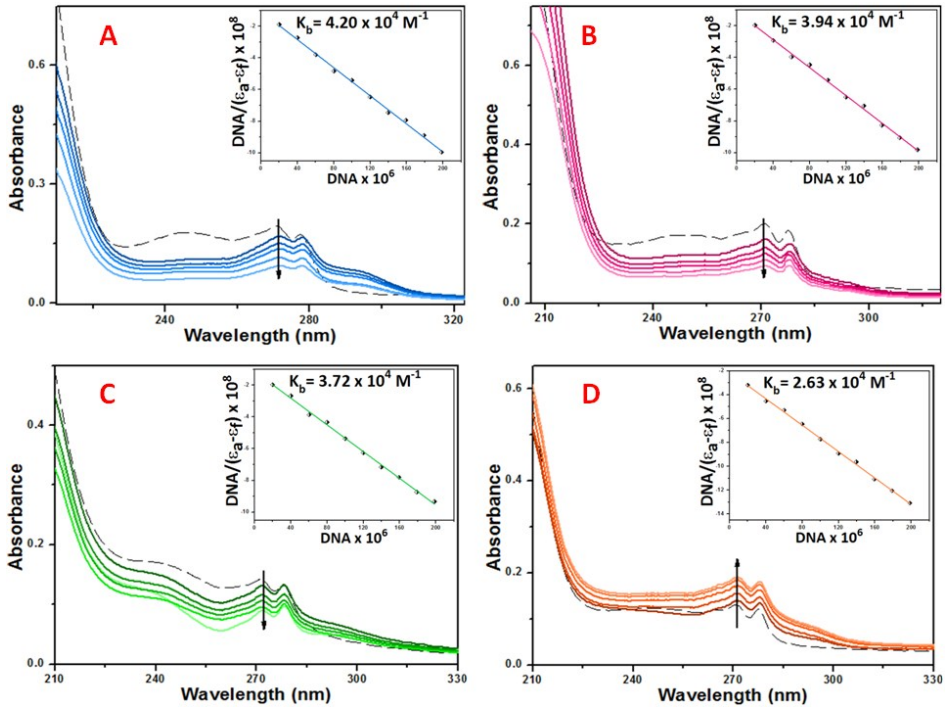

Sup. Fig. S26 UV spectra of 20 µM of (A) **C3** (B) **C4** (C) **C5** and (D) **C6** in Tris-HCl buffer in the presence of increasing amounts of CT-DNA (0–200 µM). The arrow indicates the chenges in the absorbance on addition of DNA. Inset: linear fit of [DNA]/(ε_a - ε_f) vs. [DNA].

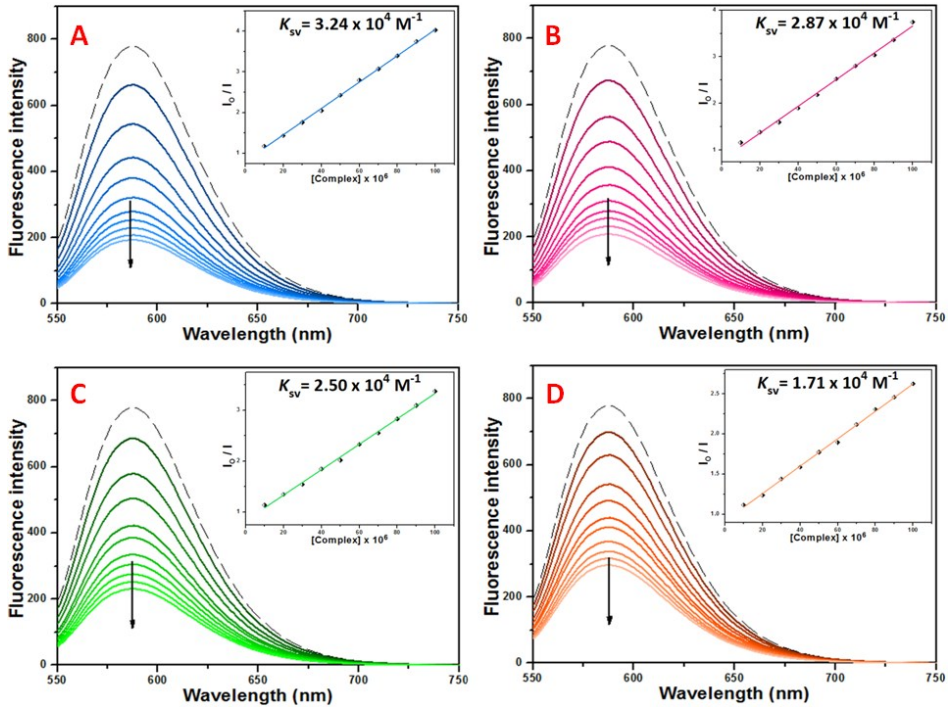

Sup. Fig. S27 Emission spectra for EB–DNA ([EB] = 20 µM, [DNA] = 20 µM) in the absence and presence of increasing amounts of (A) **C3** (B) **C4** (C) **C5** and (D) **C6**. The arrow shows the changes of intensity upon increasing amount of complexes. Inset: Plot of I_0/I versus [complex].

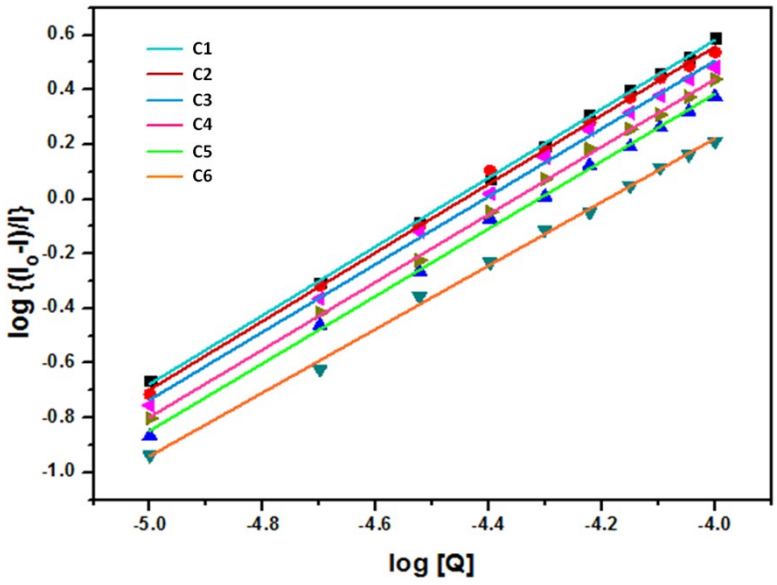

Sup. Fig. S28 Scatchard plot for DNA binding of complexes **C1**-**C6**.

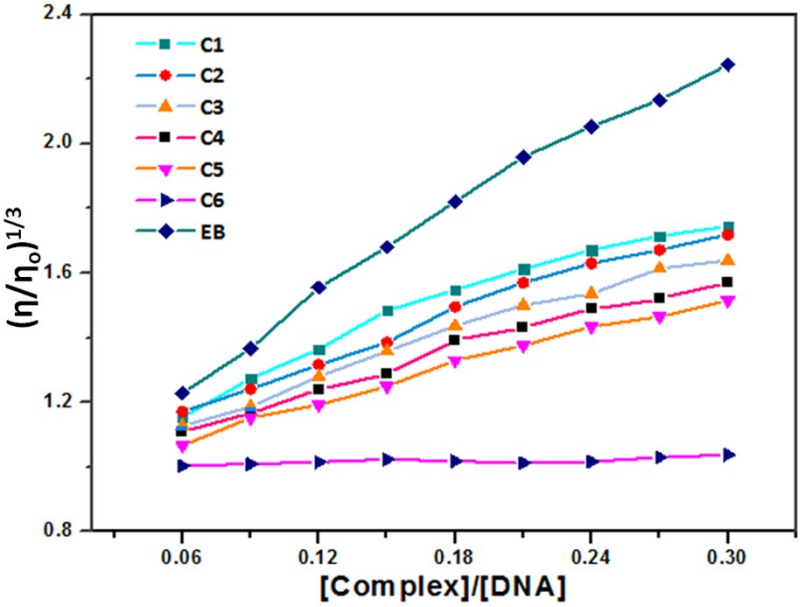

Sup. Fig. S29 Effect of increasing amounts of EB and studied Pd(II) complexes on the relative viscosity of CT-DNA at 25°C.

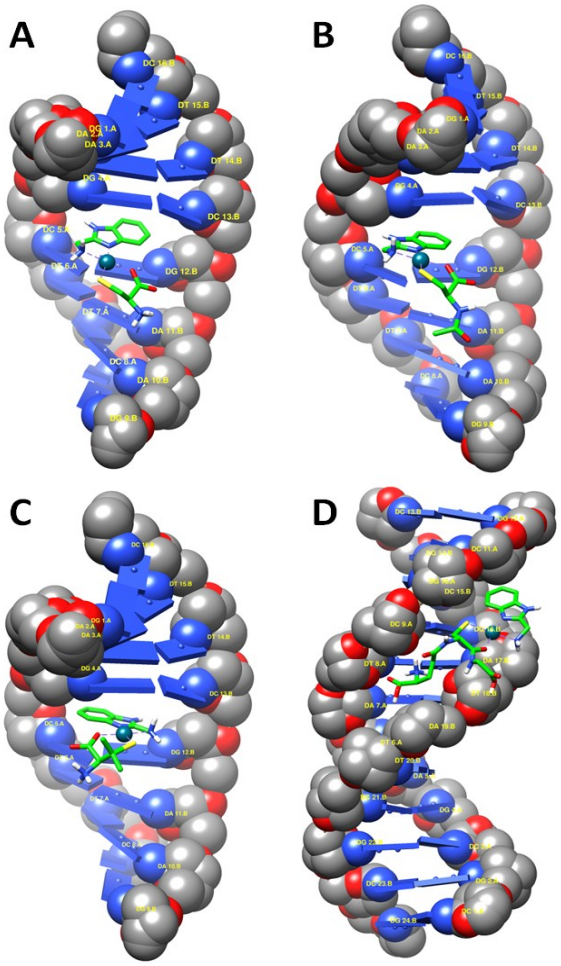

Sup. Fig. S30 Computational docking models illustrating the interactions of (A)**C3,** (B)**C4**, (C)**C5** with 1DNE and (D) **C6** with 1DSC.

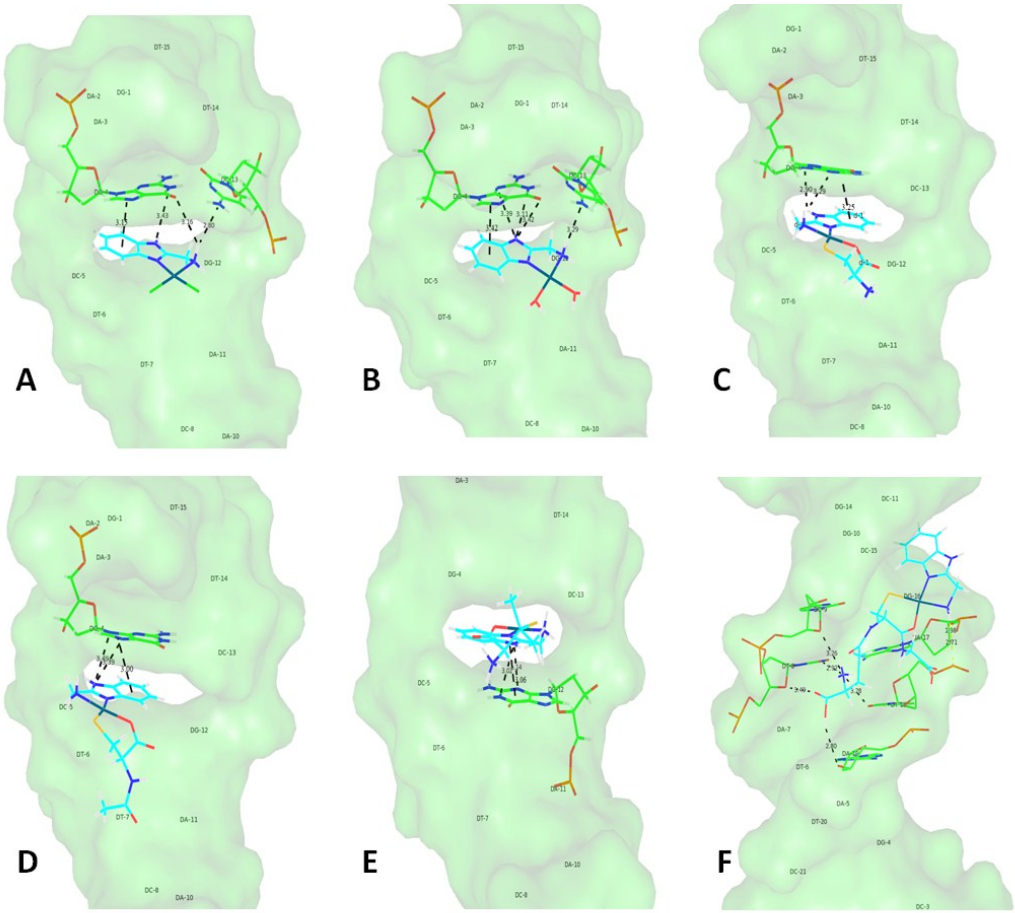

SUP. Fig. S31 Magnified view of docked model showing the interaction of DNA bases with (A) **C1**, (B) **C2**, (C) **C3**, (D) **C4**, (E) **C5** and (F) **C6**.

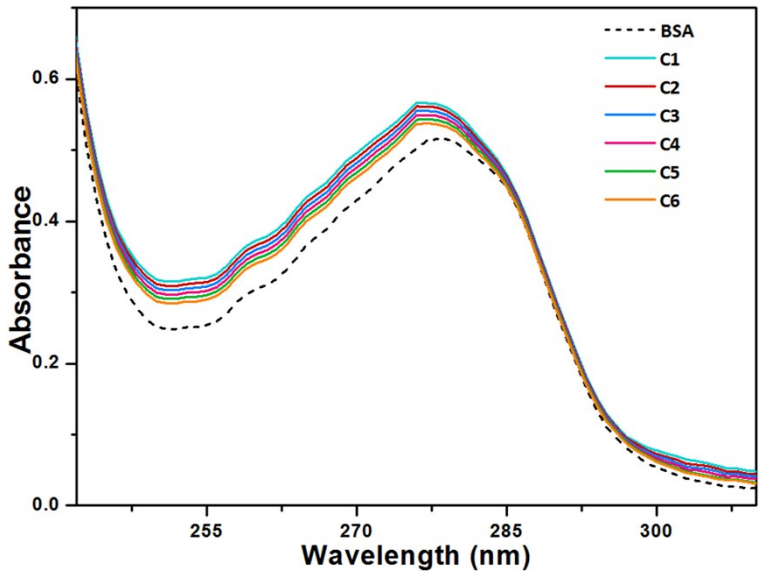

Sup. Fig. S32 Absorption spectra of BSA (10 µM) in Tris-HCl buffer in presence of the complexes **C1**–**C6** (5 µM).

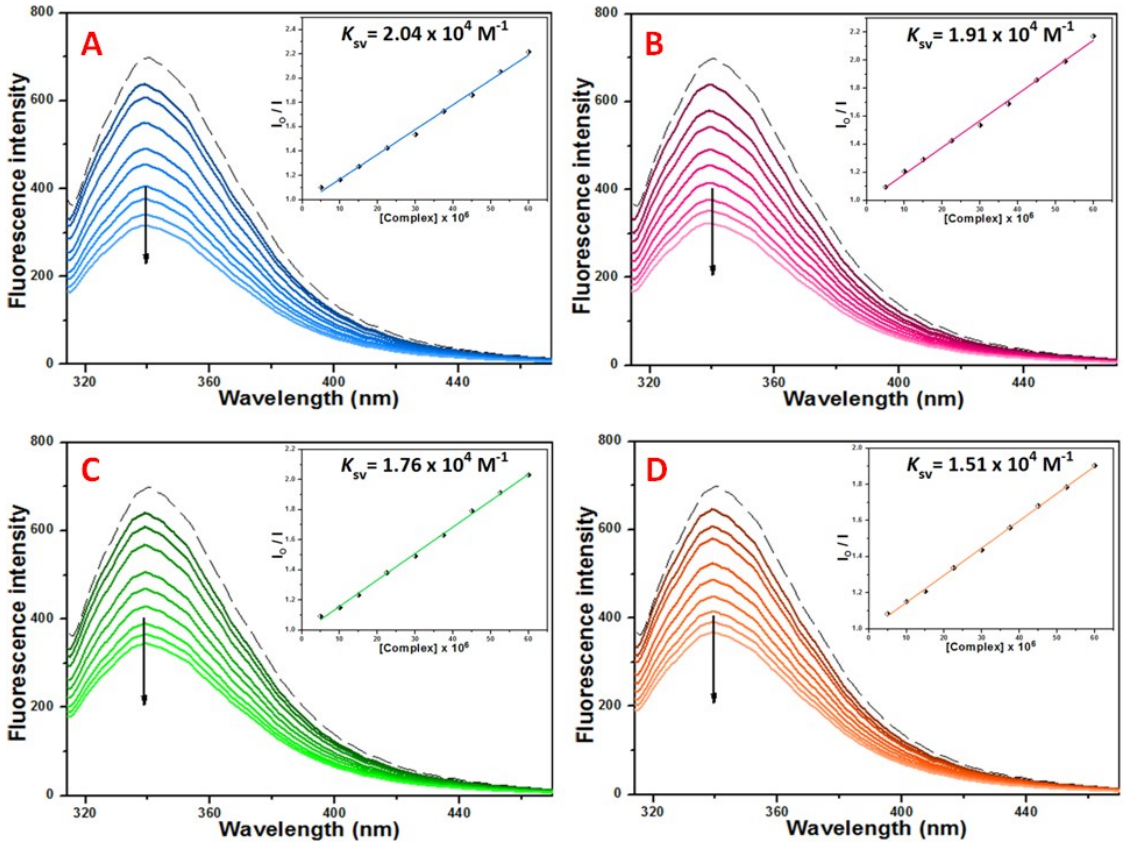

Sup. Fig. S33 Emission spectra of BSA (1.0 µM) in Tris-HCl buffer(pH 7.0) at 298 K in presence of (A) **C3**, (B) **C4**, (C) **C5** and (D) **C6**(5-60 µM). The arrow shows the emission intensity changes upon increasing complex concentration. Insets: Stern-Volmer plot showing tryptophan quenching in BSA.

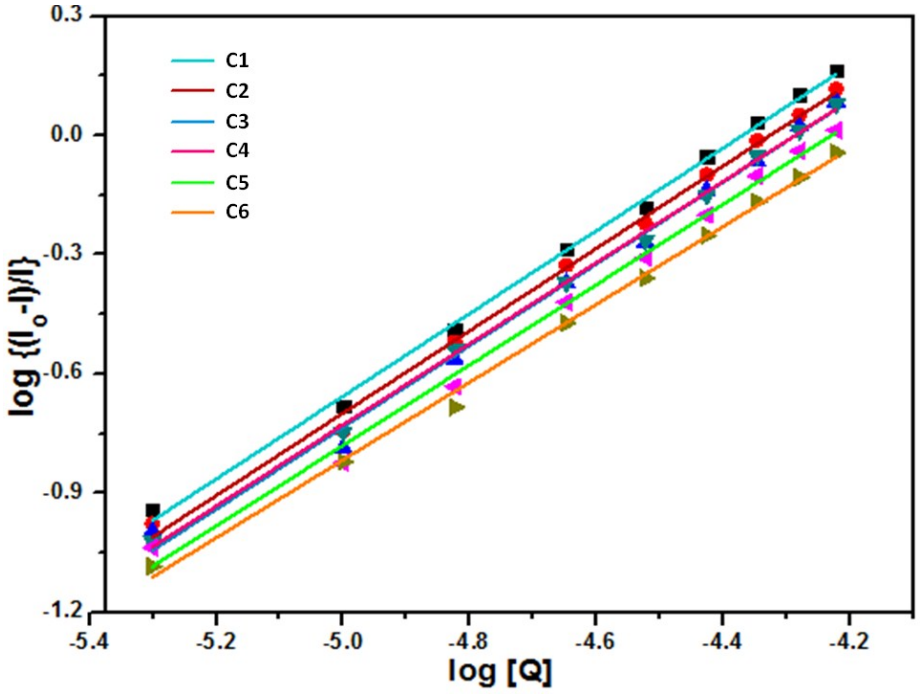

Sup. Fig. S34 Scatchard plot for BSA binding of complexes **C1**-**C6**.

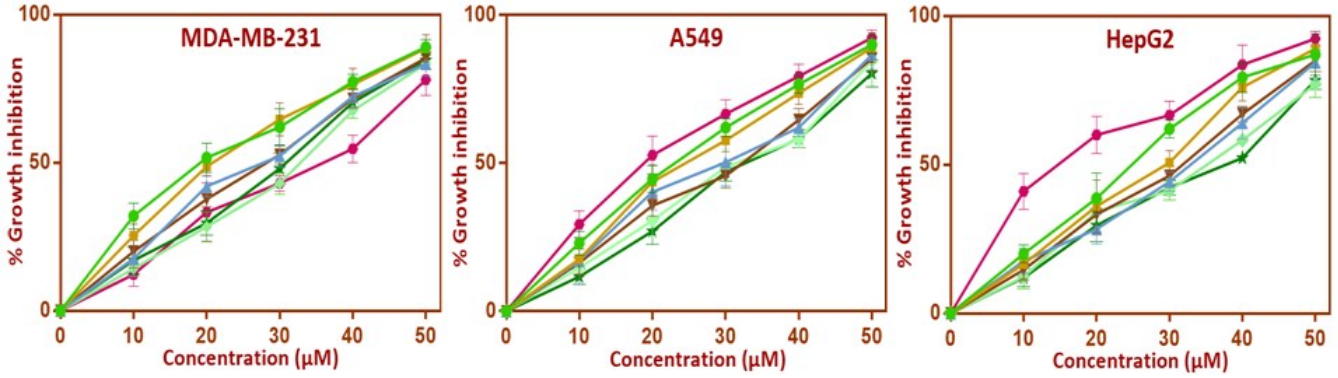

Sup. Fig. S35 Growth Inhibition (%) of MDA-MB-231, A549, and HepG2 cell lines in presence of complex **C1**-**C6** and Cisplatin (5-50 µM).

Sup. Table S1. $10^{-3} \times k_{1(obs)}$ (s^{-1}) and $k_{2(obs)}$ (s^{-1}) values at different [ligand] at different temperatures; [**C2**] = 4.71 $\times 10^{-4}$ M, pH = 4.0, ionic strength = 0.1 M $NaClO_4$ (Herein **"**± values" represent standard error values)

Ligand	Conc. ($\times 10^3$ M)	$k_{1(obs)} \times 10^{-3}$ (s^{-1})				$k_{2(obs)}$ (s^{-1})			
		15^{0}C	25^{0}C	35^{0}C	45^{0}C	15^{0}C	25^{0}C	35^{0}C	45^{0}C
L-cys	4.71	3.26±0.08	5.75±0.06	9.27±0.09	13.58±0.11	1.51±0.04	1.97±0.04	2.90±0.06	4.13±0.05
	7.06	4.24±0.03	7.38±0.05	11.84±0.07	17.22±0.08	1.55±0.07	2.01±0.03	2.94±0.04	4.20±0.10
	9.42	4.99±0.07	8.60±0.04	13.75±0.03	19.88±0.04	1.46±0.08	2.03±0.02	3.00±0.07	4.17±0.06
	11.77	5.58±0.04	9.55±0.07	15.21±0.10	21.91±0.05	1.43±0.03	1.96±0.06	3.02±0.03	4.23±0.08
	14.13	6.06±0.12	10.30±0.12	16.38±0.06	23.51±0.09	1.60±0.02	2.08±0.06	2.84±0.10	4.12±0.09
NALC	4.71	2.48±0.03	3.91±0.06	7.15±0.08	10.78±0.10	1.15±0.04	1.69±0.01	2.66±0.04	3.71±0.07
	7.06	3.38±0.08	5.07±0.09	8.95±0.07	14.11±0.06	1.23±0.02	1.74±0.04	2.61±0.06	3.66±0.05
	9.42	3.84±0.11	6.17±0.03	10.66±0.05	16.14±0.08	1.19±0.07	1.78±0.08	2.59±0.02	3.59±0.04
	11.77	4.32±0.02	6.50±0.07	12.17±0.09	17.49±0.05	1.13±0.03	1.69±0.07	2.70±0.03	3.74±0.08
	14.13	4.69±0.05	7.31±0.09	12.78±0.04	19.34±0.12	1.27±0.08	1.80±0.05	2.64±0.09	3.60±0.03
DL-pen	4.71	1.46±0.12	2.99±0.04	5.05±0.07	8.89±0.03	0.53±0.04	0.75±0.03	1.09±0.07	1.63±0.05
	7.06	2.00±0.04	3.89±0.05	6.75±0.10	11.29±0.09	0.46±0.03	0.69±0.05	1.13±0.04	1.72±0.02
	9.42	2.39±0.07	4.77±0.08	7.86±0.03	13.06±0.05	0.51±0.07	0.78±0.08	1.05±0.06	1.67±0.06
	11.77	2.68±0.09	5.20±0.09	8.80±0.05	15.00±0.06	0.40±0.05	0.80±0.02	1.02±0.03	1.63±0.08
	14.13	2.86±0.05	5.66±0.13	9.34±0.06	15.85±0.11	0.41±0.06	0.73±0.04	1.16±0.08	1.70±0.05
GSH	4.71	6.84±0.08	10.66±0.09	16.13±0.04	23.35±0.07	4.17±0.02	5.38±0.07	7.56±0.06	9.70±0.08
	7.06	8.67±0.13	13.83±0.07	20.50±0.10	28.64±0.07	4.11±0.07	5.42±0.08	7.39±0.05	9.69±0.05
	9.42	10.28±0.06	15.42±0.05	23.14±0.09	32.51±0.13	4.08±0.03	5.31±0.04	7.47±0.03	9.80±0.07
	11.77	11.27±0.05	17.13±0.08	26.26±0.07	36.58±0.09	4.01±0.06	5.43±0.03	7.50±0.04	9.65±0.06
	14.13	12.07±0.03	18.58±0.04	27.03±0.11	38.52±0.06	4.18±0.05	5.36±0.06	7.43±0.11	9.71±0.04

Sup. Table S2. Energy and composition of some selected MOs of **C3**-**C6**.

MO	C3				C4				C5				C6			
	E (eV)	% of composition			E (eV)	% of composition			E (eV)	% of composition			E (eV)	% of composition		
		Pd	Ambim	L		Pd	Ambim	L		Pd	Ambim	L		Pd	Ambim	L
L+3	0.01	50	31	19	0.14	12	82	6	0.01	47	22	31	-0.17	2	1	97
L+2	-0.18	29	4	67	0.08	54	22	24	-0.24	32	5	63	-0.42	7	3	90
L+1	-1.06	2	98	0	-1.01	1	98	0	-1.07	1	98	0	-1.14	1	98	1
LUMO	-2.46	51	20	29	-2.22	51	19	31	-2.42	51	20	29	-2.51	51	20	29
HOMO	-5.98	20	8	73	-5.73	18	4	78	-5.94	19	6	75	-5.92	1	0	99
H-1	-6.69	4	86	9	-6.57	39	39	22	-6.68	6	86	9	-5.98	15	1	84
H-2	-6.76	5	93	2	-6.62	28	45	27	-6.77	7	91	2	-6.13	0	0	100
H-3	-6.85	71	10	19	-6.72	8	34	57	-6.84	67	15	18	-6.29	0	0	99

Sup. Table S3. Occupancy (e) and polarity (%) of natural bond orbitals (NBOs) and hybrids calculated[(a)] for **C4-C6**.

System	NBO Orbital [(b)]	Occupancy	Polarity [(c)]	NBO Hybrid	Atomic Orbitals [(d)]
	σPt-S	1.83058	22.47 (Pd)	$sd^{2.05}$	s(25.30%) p(22.77%) d(51.93%)
C4			77.33 (S)	$sp^{7.08}$	s(12.37%) p(87.63%)
	LP(O1)	1.72674	-	$sp^{4.19}$	s(17.04%) p(71.40%)
	LP(N2)	1.68079	-	$sp^{4.25}$	s(19.05%) p(80.95%)
	LP(N3)	1.65421	-	$sp^{6.21}$	s(14.38%) p(89.30%)
	σPt-S	1.96833	35.87 (Pd)	$sd^{5.40}$	s(14.15%) p(9.41%) d(76.45%)
C5			64.13 (S)	$sp^{7.61}$	s(11.62%) p (88.38%)
	LP(O1)	1.67459	-	$sp^{5.71}$	s(14.90%) p(85.10%)
	LP(N2)	1.67554	-	$sp^{5.20}$	s(16.12%) p(83.88%)
	LP(N3)	1.65142	-	$sp^{2.69}$	s(27.13%) p(72.86%)
	σPt-S	1.98535	22.09 (Pd)	$sd^{8.40}$	s(10.00%) p(5.95%) d(84.05%)
C6			77.91 (S)	$sp^{3.71}$	s(22.08%) p(77.78%)
	LP(O1)	1.70257	-	$sp^{5.54}$	s(15.30%) p(84.70%)
	LP(N2)	1.63588	-	$sp^{8.27}$	s(10.78%) p(89.16%)
	LP(N3)	1.65142	-	$sp^{6.01}$	s(12.06%) p(72.48%)

(a) Calculations performed at B3LYP/ LANL2DZ /6-31G(d)/6-31G+(d) level of theory. (b) LP(N/O) is a valence lone pair orbital on nitrogen/oxygen atom. (c) Values for A–B sigma molecular orbital. (d) Percentage contribution of atomic orbitals in NBO hybrid.

Sup. Table S4. Selected vertical excitations calculated by TDDFT/B3LYP/6-31G(d)/6-31G+(d)/LANL2DZ /CPCM/water for **C3**-**C6**.

Complex	E_{ex} (eV)	λ_{ex} (nm)	λ_{max} (expt.) (nm)	Osc. Strength (*f*)	Key transitions	Assignments
C4	6.09	203	204	0.2562	H-14→LUMO (18%), H-1→L+3 (18%), H-13→LUMO (14%)	Ambim(π)/NALC(π)→Pd(dπ), LMCT
	5.25	236	-	0.2449	HOMO→L+4 (36%), HOMO→L+2 (21%), H-11→LUMO (13%), H-8→LUMO (11%)	Ambim(π)→Pd(dπ)/NALC(π*), LMCT/LLCT
	4.65	267	270 278	0.2547	H-8→LUMO (45%), H-11→LUMO (15%)	Ambim(π)→Pd(dπ)/NALC(π*), LMCT/LLCT
	3.92	316	-	0.0756	H-3→LUMO (37%), H-4→LUMO (25%), H-2→LUMO (17%), H-6→LUMO (12%)	NALC(π)/Ambim(π)→Pd(dπ), LMCT
C5	5.76	215	210	0.1399	H-5→LUMO (54%), H-8→LUMO (17%)	Ambim(π)/DL-pen(π)→Pd(dπ), LMCT
	5.00	248	244	0.1881	H-2→L+1 (53%), H-3→L+1 (35%)	Pd(dπ)/DL-pen(π)→Ambim(π*), MLCT/LLCT
	4.50	275	272 278	0.1436	H-11→LUMO (45%), H-12→LUMO (19%)	DL-pen(π)→Pd(dπ)/Ambim(π*), LMCT/LLCT
C6	5.66	219	223	0.1168	H-7→L+2 (58%), H-9→L+2 (30%)	Ambim(π)/Pd(dπ) → GSH(π*) LLCT/MLCT
	5.03	250	272	0.1747	H-10→LUMO (73%)	GSH(π)/Pd(dπ)→Ambim(π*), LLCT/MLCT
	4.25	291	278	0.1965	H-8→L+1 (67%), H-7→L+4 (15%)	GSH(π)→Pd(dπ)/Ambim(π*), LMCT/LLCT

Sup. Table S5. Band shift (nm) and free energy (kJ mol^{-1}) of DNA binding by absorption titration.

Complex	Band shift Δλ (nm)	ΔG (kJ mol^{-1})
C1	7	-27.18
C2	4	-26.99
C3	6	-26.37
C4	7	-26.22
C5	6	-26.07
C6	-2	-25.22

Sup. Table S6 A few hydrogen bonding interactions and the binding free energy of the most stable docking conformations for complexes **C1**–**C6** docked into DNA.

Complex	H-bonding			ΔG (kJ mol^{-1})
	Donor (D–H)	Acceptor (H···A)	H···A (Å)	
C1	N_{im} (Ambim)	N (DC-13)	2.80	-26.36
	N_{im} (Ambim)	N (DG-4)	3.43	
	N_{im} (Ambim)	O (DG-4)	3.16	
C2	N_{im} (Ambim)	N (DG-4)	3.39	-25.94
	N_{im} (Ambim)	O (DG-4)	3.11	
	N_{am} (Ambim)	N (DC-13)	3.29	
C3	N_{im} (Ambim)	N (DG-4)	2.90	-25.10
	N_{im} (Ambim)	N (DG-4)	3.29	
C4	N (DG-4)	N_{im} (Ambim)	3.39	-25.52
	N (DG-4)	N_{im} (Ambim)	3.49	
C5	N (DG-12)	N_{im} (Ambim)	3.02	-24.69
	N (DG-12)	N_{im} (Ambim)	3.06	
C6	O (GSH)	O (DA-19)	2.80	-25.10
	O (DT-8)	O (GSH)	3.49	
	N (DT-8)	N (GSH)	2.92	
	O (DT-18)	N (GSH)	3.28	

Sup. Table S7. IC_{50} values (in μM) of the complexes **C1**-**C6** and cisplatin on different cancer cell lines for 48 hrs incubation.

Complex	IC_{50} (μM)		
	MDA-MB-231	A549	HepG2
C1	19.4 ± 0.5	23.5 ± 0.8	25.2 ± 0.5
C2	21.2 ± 0.6	24.1 ± 1.0	30.1 ± 0.9
C3	26.0 ± 0.9	29.7 ± 0.7	33.2 ± 0.4
C4	27.9 ± 1.2	31.2 ± 0.6	31.7 ± 0.9
C5	33.4 ± 0.7	30.8 ± 0.4	38.0 ± 1.3
C6	31.5 ± 0.6	32.3 ± 0.9	35.4 ± 1.0
Cisplatin	37.1 ± 1.1	19.0 ± 0.7	14.3 ± 0.8

ESI Equation S1. Wolfe-Shimer equation

The intrinsic binding constant (k_b) for all the studied complexes has been evaluated by using Wolfe-Shimer equation [1].

$$[DNA]/ [\varepsilon_a-\varepsilon_f] = [DNA]/ [\varepsilon_b-\varepsilon_f] + 1/\{K_b\times [\varepsilon_b-\varepsilon_f]\}$$

Where, [DNA] is the concentration of CT-DNA in base pairs, ε_a, ε_f, ε_b correspond to the extinction coefficient of observed ($A_{obsd}/[M]$), free complex and of the complex when fully bound to CT-DNA respectively. $[DNA]/(\varepsilon_a- \varepsilon_f)$ versus [DNA] has been plotted and the slope to intercept ratio gives the magnitude of K_b for each of the complexes.

ESI Equation S2. Free energy of binding

ESI Equation 2 has been used to calculate the free energy (ΔG) of binding for complex-DNA adduct formation [2].

$$\Delta G = -RT \ln K_b$$

ESI Equation S3. Stern–Volmer equation

$$I_0/I = 1 + K_{sv}[Q] = 1 + k_q\tau_o$$

I_0 and I are the fluorescence intensities at 587 nm in absence and presence of the quencher 'Q' [Pd(II) complexes] respectively. K_{sv},the linear Stern-Volmer quenching constant [3] was determined by linear regression of a plot of I_o/I vs [Q]. k_q is the bimolecular quenching constant and τ_0 is the lifetime of the chromophore in the absence of the quencher ($\tau_o = 23 \times 10^{-9}$ s for EB-bound DNA).[4]

ESI Equation S4. Scatchard equation

$$\log (I_0-I)/I = \log K_F + n \log [Q]$$

log (I_0 - I)/I versus log [Q] has been plotted and fitted linearly. Intercept will provide the binding constant K_F. The number of binding sites per nucleotide i.e., 'n' has been obtained from the slope [5].

References

[1] A. Wolfe, G.H. Shimer and T. Meehan, *Biochem.*, 1987, **26**, 6392.

[2] K. Karami, Z. M. Lighvan, S. A. Barzani, A. Y. Faal, M. Poshteh-Shirani, T. Khayamian, V. Eignerc and M. Dusˇek, ***New J. Chem.*,** 2015, **39,** 8708.

[3] H. Akbaş, A. Karadağ, A. Aydın, A. Destegül and Z. Kılıç, *J. Mol. Liq.*, 2017, **230**, 482.

[4] D. P. Heller and C. L. Greenstock, *Biophys. Chem.*, 1994, **50**,305.

[5] J. Min, X. M. Meng-Xia, Z. Dong, L. Yuan, L. Xiao-Yu and C. Xing, *J. Mol. Struct*., 2004, **692**, 71.